Structures of fine particles in cylindrical plasmas: Theory, simulations, and experiments under gravity and microgravity

H. Totsuji[1,3], K. Takahashi[2], S. Adachi[3], C. Totsuji[4], M. Tonouchi[2]

[1]*Okayama University, Okayama, Japan,* [2]*Kyoto Institute of Technology, Kyoto, Japan,*
[3]*JAXA/ISAS, Tsukuba, Japan,* [4]*Kogakuin University, Tokyo, Japan*

Behavior of fine particles in cylindrically symmetric plasmas is analyzed. Self-consistent distributions are obtained and structure formations are shown.

Introduction

Fine particles in plasmas are unique in the respect that strong coupling between particles is realized and kinetic level observations are possible. The only drawback is the effect of gravity and ideal experiments need the microgravity environment. Experiments on ISS by the MPE/JIHT have revealed many important aspects of strongly coupled systems. Next to PK-3 Plus presently operated, PK-4 is planned. Since the latter has a long discharge tube, physical phenomena in cylindrically symmetric systems are expected to be newly observed. We are investigating such phenomena which will help us to understand physics of strong coupling and could be proposed as candidates for experiments in PK-4[1, 2].

Theory and Simulation

fluid limit

In this limit, the behavior of fine particle plasmas is described by the diffusion equations. For electrons(e), ions(i), and fine particles(p), we have

$$\frac{\partial}{\partial t}n_{(e,i,p)}+\mathrm{div}[-D_{(e,i,p)}\ \mathrm{grad}\ n_{(e,i,p)}-\mu_{(e,i,p)}n_{(e,i,p)}\mathbf{E}]=\frac{\delta n_{(e,i,p)}}{\delta t}. \tag{1}$$

Here $D_{(e,i,p)}$ and $\mu_{(e,i,p)}$ are the diffusion coefficient and the mobility of each species, respectively. On the right-hand sides, the generation or loss per unit volume and time is expressed by $\delta n_{(e,i,p)}/\delta t$. The electric field $\mathbf{E}$ is related to the charge density by the Poisson's equation as

$$\varepsilon_0\ \mathrm{div}\ \mathbf{E}=(-Qe)n_p+e(n_i-n_e). \tag{2}$$

We investigate the stationary solution ($\partial n_{(e,i,p)}/\partial t=0$). As for the plasma production, we assume

$$\frac{\delta n_e}{\delta t}=\frac{\delta n_i}{\delta t}=\alpha n_e \quad \text{and} \quad \frac{\delta n_p}{\delta t}=0, \tag{3}$$

where α is a constant. The boundary conditions at the wall are $n_e(\mathrm{wall})=n_i(\mathrm{wall})=0$. For particles, $n_p(\mathrm{wall})$ is sufficiently small but not exactly zero. (Mathematically, $\delta n_p/\delta t=0$ and $n_p(\mathrm{wall})=0$ lead to the trivial stationary solution $n_p=0$ everywhere.)

Without fine particles, it is useful to rewrite diffusion equations for electrons and ions into the form controlled by the ambipolar diffusion coefficient $D_a = (\mu_i D_e + \mu_e D_i)/(\mu_e + \mu_i)$ noting the condition of quasi-neutrality. With fine particles, however, it is not possible to simply apply the ambipolr diffusion equation except for the case of negligible charge density of particles. Since particles are highly (negatively) charged, we have to take into account their contribution self-consistently even if their density is much smaller than electrons or ions.

We assume the cylindrical symmetry and numerically solve (1) and (2). We start from the symmetry axis where all densities are finite and search for solutions which satisfy the boundary conditions at the wall, leaving the charge non-neutrality at the axis as an adjustable parameter. The radius of distribution is determined by the condition that n_e and n_i becomes zero *at the same position* which is satisfied only for a unique value of the adjustable parameter. Since we have large dimensionless parameters, such as T_e/T_i, D_e/D_i, and Q, numerical solution of these equations is a challenge.

Top panel in Fig.1 shows the distribution of electrons and ions without fine particles in comparison with the result of ambipolar diffusion equation (broken line). As expected, densities of electrons and ions are almost equal except for the domain of the sheath on the periphery which is reproduced by our self-consistent solutions.

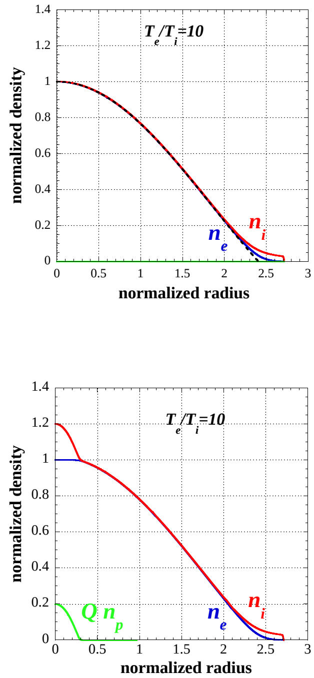

Figure 1: Distribution with (bottom) and without (top) fine particles.

An example of solutions with fine particles are shown in bottom panel in Fig.1. The characteristic features of these results are summarized as follows: (a) Fine particles are distributed around the axis, (b) in the domain where particles are distributed, the quasi-charge-neutrality is satisfied by the increased density of ions while the electron density is almost constant.

effect of discreteness

When we take the discreteness of particles into account, there appears the particle-particle and particle-plasma (electrons and ions) correlation. As a result, the interaction between particles is modified into the Yukawa repulsive potential $v(r)$. In the case of uniform system, the interaction energy per particle is expressed by the pair distribution function $g(r)$ as[3]

$$\frac{1}{2} n_p \int d\mathbf{r} v(r)[g(r) - 1]. \quad (4)$$

Note that, since the interaction energy comes from the effect of discreteness, we have to subtract unity from $g(r)$: The interaction energy is zero in the state of the uniform (or random) distribution (the fluid limit) $g(r) = 1$ due to charge neutrality. This subtraction can also regarded as the interaction with the background charges which neutralize the charge of particles[3].

Also in the non-uniform case, the effective interaction energy between particles should reduce to zero when the discreteness of particles is neglected. This condition is realized by subtracting the interaction energy with the Yukawa particles distributed according to the fluid limit distribution, or equivalently, by adding the interaction with the 'background' Yukawa particles. We can thus simulate the effect of discreteness by including the one-body potential of the (Yukawa) interaction with (exactly) neutralizing background charges in addition to mutual Yukawa repulsions[3].

When the particle distribution in the fluid limit is uniform in a cylinder, the effect of discreteness appears as the formation of almost equally spaced shells as expressed by simple and accurate formulas[1]. An example is shown in Fig.2. Even in the case where the distribution in the fluid limit is not uniform, the distribution near the axis can be regarded as uniform and we may apply our previous results in this domain.

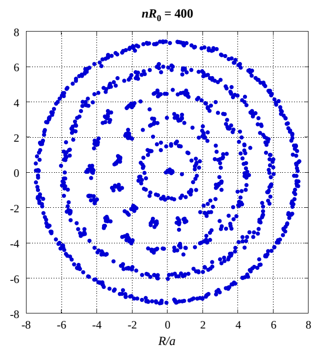

Figure 2: Shell structure in the uniform case.

In Fig.3, we show some examples of the results of simulations at low temperatures where the potential due to distribution in the fluid limit is regarded as a parabola and the gravitation perpendicular to the axis exists. With the increase of the gravitational field, the shells are compressed vertically. The shells (layers) keep their identity at least in these simulations.

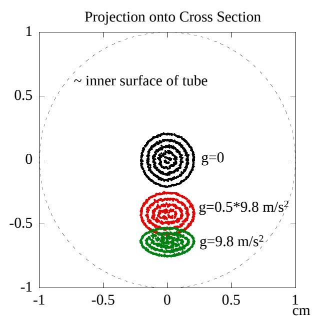

Figure 3: Shell structures under gravity.

Experiments on the Ground and in Parabolic Flights

We have constructed the apparatus PK-4J (shown in Fig.4) with the structure similar to PK-4 and performed experiments on the ground and in the parabolic flights (PF). The gas is Ar and the polarity of DC discharge ($\sim$ 1 kV) is switched with 1 kHz. Typically, the pressure is 15 $\sim$ 40 Pa and plasma parameters are (expected, not yet established) $n_e \sim 10^8\text{cm}^{-3}$ and $T_e \sim$ a few eV.

In PF in 2011, fine particles are distributed around the symmetry axis as shown in Fig.5. The diameter of distribution is 0.57 cm in the discharge tube of diameter 3 cm. However, the position of each fine particle is not resolved. In PF in 2012, the images of particles are digitized.

Examples of positions are shown in Fig.6. The cross section is approximately circular and there seem to exist some layer structures parallel to the right-to-left direction.

In most cases of PF, the system of injected particles flows along the axis and we have not succeeded to suppress. We suspect the apparent left-to-right structures are due to errors in digitization of CCD image induced by the axial flow.

On the ground, the cylindrical part is placed horizontally and we have better control of the flow. An example of positions is shown in Fig.6. We observe the shell structures vertically compressed by gravity similarly to the result of numerical simulations.

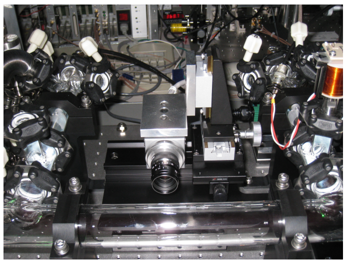

Figure 4: PK-4J.

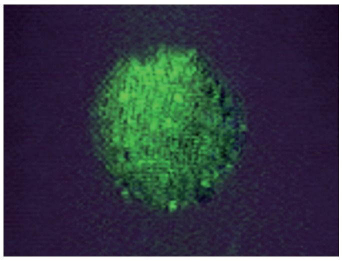

Figure 5: Cross section under microgravity.

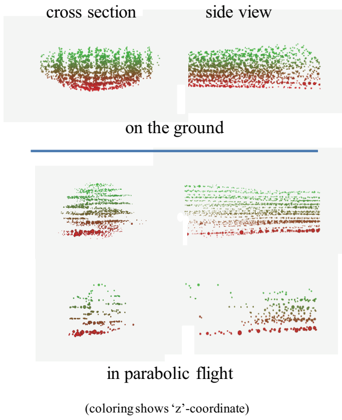

Figure 6: Particle distribution in experiments.

Conclusion

We have developed the theory on the fine particle plasmas with cylindrical symmetry and performed experiments on the ground and in parabolic flights. Overall characteristics of predicted self-consistent particle distribution and structure formations are in accordance with experimental observations. We need, however, further improvement both theoretical and experimental to facilitate accurate comparisons and identify parameters of fine particle plasmas.

The authors deeply thank the MPE/JIHT group lead by Professor G. E. Morfill and Professor V. E. Fortov for chances of ISS experiments by PK-3 Plus and useful information of planned apparatus PK-4. They thank JAXA for financial support as one of Working Group activities. H.T. is supported also by the Grant-in-Aid for Scientific Research from JSPS.

References

[1] H. Totsuji and C. Totsuji, Phys. Rev. E, **84**, 015401(R)(2011)

[2] H. Totsuji and C. Totsuji, J. Phys.: Conference Series **327**, 012037(2011); H. Totsuji and C. Totsuji, *Dusty/Complex Plasmas: Basic and Interdisciplinary Research*, AIP Conference Proceedings **1397**, 92(2011)

[3] H. Totsuji, C. Totsuji, T. Ogawa, and K. Tsuruta, Phys. Rev. E, **71**, 045401(R)(2005); H. Totsuji, T. Ogawa, C. Totsuji, and K. Tsuruta, Phys. Rev. E, **72**, 036406(2005)